

# Excellence in Chemistry Research

## Announcing our new flagship journal

- Gold Open Access
- Publishing charges waived
- Preprints welcome
- Edited by active scientists



## Meet the Editors of *ChemistryEurope*



**Luisa De Cola**  
Università degli Studi  
di Milano Statale, Italy



**Ive Hermans**  
University of  
Wisconsin-Madison, USA



**Ken Tanaka**  
Tokyo Institute of  
Technology, Japan

# Tuning the Bioactivity of Tensioactive Deoxy Glycosides to Structure: Antibacterial Activity Versus Selective Cholinesterase Inhibition Rationalized by Molecular Docking

Alice Martins,<sup>[a]</sup> Maria S. Santos,<sup>[a]</sup> Catarina Dias,<sup>[a]</sup> Patrícia Serra,<sup>[a]</sup> Vasco Cachatra,<sup>[a]</sup> João Pais,<sup>[a]</sup> João Caio,<sup>[a]</sup> Vítor H. Teixeira,<sup>[a]</sup> Miguel Machuqueiro,<sup>[a]</sup> Marta S. Silva,<sup>[a]</sup> Ana Pelerito,<sup>[b]</sup> Jorge Justino,<sup>[c]</sup> Margarida Goulart,<sup>[c]</sup> Filipa V. Silva,<sup>[c]</sup> and Amélia P. Rauter\*<sup>[a]</sup>

*Dedicated to the centenary of the Portuguese Chemical Society on the occasion of the 6th Spanish Portuguese Japanese Organic Chemistry Symposium*

**Keywords:** Synthetic methods / Medicinal chemistry / Glycosides / Surfactants / Biological activity / Molecular docking

New octyl/dodecyl 2,6-dideoxy-D-*arabino*-hexopyranosides have been synthesized by a simple but efficient methodology based on the reaction of glycals with alcohols catalysed by triphenylphosphane hydrobromide, deprotection, regioselective tosylation and reduction. Their surface-active properties were evaluated in terms of adsorption and aggregation parameters and compared with those of 2-deoxy-D-glycosides and 2,6-dideoxy-L-glycosides. Deoxygenation at the 6-position led to a decrease in the critical micelle concentration, and an increase in the adsorption efficiency ( $pC_{20}$ ) promoting aggregation more efficiently than adsorption. With regard to the antibacterial activity, dodecyl 2,6-dideoxy- $\alpha$ -L-*arabino*-hexopyranoside was the most active compound towards *Bacillus anthracis* (MIC 25  $\mu$ M), whereas its enantiomer exhibited a MIC value of 50  $\mu$ M. Both 2,6-dideoxy glycosides were active towards *Bacillus cereus*, *Bacillus subtilis*, *Enterococcus faecalis* and *Listeria monocytogenes*. In contrast, none of the 2-deoxy glycosides was significantly active. These results

and the data on surface activity suggest that aggregation is a key issue for antimicrobial activity. Beyond infection, Alzheimer's disease also threatens elderly populations. In the search for butyrylcholinesterase (BChE) selective inhibition, 2-deoxy glycosides were screened in vitro by using Ellman's assay. Octyl 2-deoxy- $\alpha$ -D-glycoside was found to be a BChE selective inhibitor promoting competitive inhibition. Docking studies supported these results as they pinpoint the importance of the primary OH group in stabilizing the BChE inhibitor complex. A size-exclusion mechanism for inhibition has been proposed based on the fact that acetylcholinesterase (AChE) exhibits several bulky residues that hinder access to the active-site cavity. This work shows how the deoxygenation pattern, configuration and functionality of the anomeric centre can tune physical and surface properties as well as the bioactivity of these multifunctional and stereochemically rich molecules.

## Introduction

Sugar-based surfactants are gaining increasing attention due to their biological and medicinal applications. Varia-

tions in the nature of the sugar and hydrocarbon tail length determine the self-organization properties and therefore applications of the resulting surfactant.<sup>[1]</sup> These molecules are also known for their biocompatibility, low toxicity and fast biodegradation, which make them very attractive for industrial applications.<sup>[2]</sup>

The active site of many pharmacologically active amphiphilic molecules is frequently the plasma membrane. When the target is intracellular, the interaction with this first barrier may determine their activity. Thus, the interaction of potential drugs with membranes plays a fundamental role by either blocking permeation, inducing solubilization<sup>[3]</sup> or modifying the membrane structure. In addition, membrane protein conformation disruption alters important functions such as transport and energy generation.<sup>[4]</sup> Surface-active drugs with very different chemical structures are known to

[a] Centro de Química e Bioquímica, Faculdade de Ciências da Universidade de Lisboa, Ed. C8, Piso 5, Campo Grande, 1749-016 Lisboa, Portugal  
Fax: +351-21-7500088  
E-mail: aprauter@fc.ul.pt  
Homepage: <http://carbohydrate.cqb.fc.ul.pt/Profiles/aprauter.pdf>

[b] Instituto Nacional de Saúde Doutor Ricardo Jorge, Av. Padre Cruz, 1649-016 Lisboa, Portugal

[c] Escola Superior Agrária de Santarém, Instituto Politécnico de Santarém, Quinta do Galinheiro, 2001-904 Santarém, Portugal

Supporting information for this article is available on the WWW under <http://dx.doi.org/10.1002/ejoc.201201520>.

self-associate and bind to membranes, acting in a detergent-like manner, accumulating and affecting the organization and thermotropic properties of lipid bilayers.<sup>[3,5,6]</sup> Traditional hard cationic surfactants exhibit high antimicrobial activity due to their membrane disruptive nature, but can damage mammalian cells upon long exposure, whereas neutral surfactants are known for their soft antimicrobial properties.<sup>[7]</sup>

Our previous studies on alkyl deoxy-hexopyranosides of the D and L series in their  $\alpha$ - and  $\beta$ -anomeric configurations<sup>[8,9]</sup> have shown that high surface activity is a pre-requisite for their antimicrobial activity, but the specificity appears to be linked to the anomeric configuration of the sugar and to the deoxygenation pattern.<sup>[8,9]</sup> They are active towards *Listeria monocytogenes* and *Enterococcus faecalis*, which cause life-threatening infections in humans, particularly affecting older individuals who are more susceptible to infections, especially in hospitals, where high levels of antibiotic resistance are found. A potent activity towards *Bacillus* spp. was also found, in particular towards *Bacillus cereus*, a pathogenic microbe, the genome of which is very similar to that of *Bacillus anthracis*,<sup>[10]</sup> a well-known bio-terrorism agent responsible for anthrax infections in livestock and humans. Recently, 2,4-diaminopyrimidines were reported to inhibit this microbe.<sup>[11]</sup> As a result of the reported microbial resistance to this family of antibiotics and to many other available therapeutics,<sup>[12]</sup> the synthesis of new antimicrobial agents with new mechanisms of action for the effective treatment of infectious diseases is mandatory. Herein, we present the first results concerning the antimicrobial activity of a new family of antibiotics based on alkyl deoxy glycosides synthesized by our group<sup>[13]</sup> towards three strains of *B. anthracis*.

Other age-associated pathologies include neurodegenerative disorders, namely Alzheimer's disease (AD), which, it is estimated, will affect 70 million people in 2050 if the lack of an efficient treatment persists.<sup>[14]</sup> Its treatment is presently based on acetylcholinesterase (AChE) or AChE and butyrylcholinesterase (BChE) dual inhibitors, and is effective only in the early-to-middle stages of the disease. The activity of AChE in the brains of AD patients decreases whereas that of BChE gradually increases up to 40–90%.<sup>[15]</sup> Moreover, selective BChE inhibition results in a concomitant increase in brain acetylcholine levels and a decrease in Alzheimer's  $\beta$ -amyloid in rodents.<sup>[16]</sup> However, the impact of BChE inhibition on cognitive dysfunction remains to be determined.<sup>[17]</sup> Selective BChE inhibitors have been considered an attractive therapy for AD patients but none of them has reached the market yet. Hence, the search for new molecular entities that exhibit this activity remains a challenge and our research program on healthy ageing has involved the screening of these new compounds for this activity.

The results obtained so far for the alkyl 2-deoxy glycosides of the D series and for the 2,6-dideoxy analogues of the L series suggest that this family of compounds should be further explored and that, in particular, the study of the 2,6-dideoxy analogues of the D series is imperative. In this work we have synthesized new alkyl 2,6-dideoxy glycosides

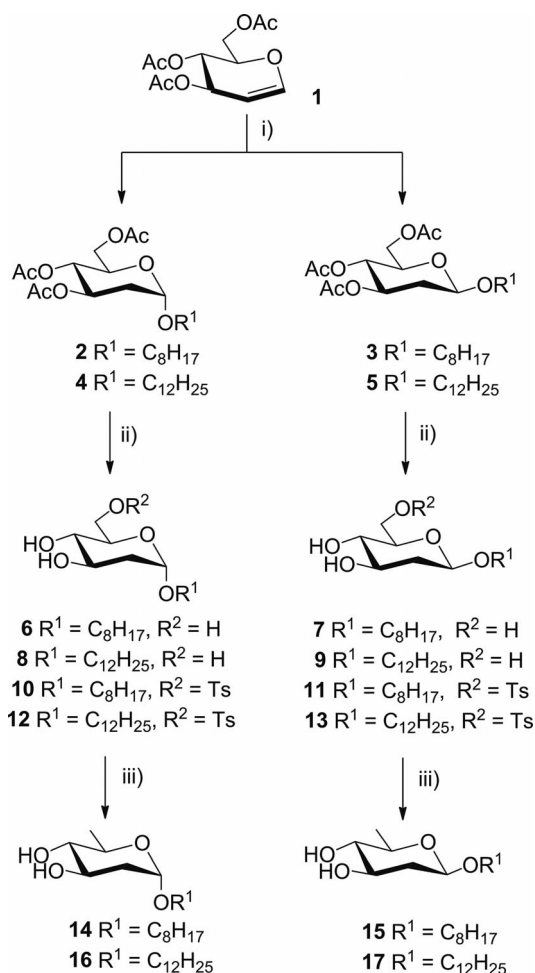
of the D series by a simple but efficient methodology and evaluated their surface-active properties and antimicrobial activities. Furthermore, in vitro screening for AChE and BChE inhibition by alkyl 2-deoxy and alkyl 2,6-dideoxy glycosides was carried out and docking studies were performed to rationalize the selective inhibition observed and to elucidate the stereoselectivity and binding properties of the active molecules.

The results reported herein clearly demonstrate that simple and easily achieved structural modifications to the glycon enable tuning of the glycoside bioactivity, thus enhancing the importance of these multifunctional and stereochemically rich molecules.

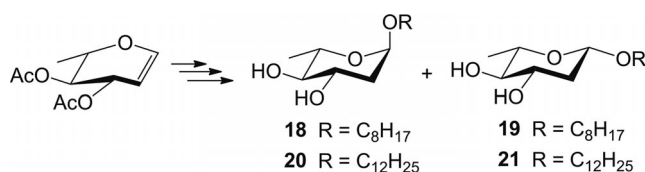
## Results and Discussion

### Synthesis

The 2-deoxy glycosides were synthesized in good yields by the reaction of glycols with fatty alcohols in the presence of triphenylphosphane hydrobromide (TPHB).<sup>[9,18]</sup> With this catalyst, the Ferrier products, which result from reaction of acetylated glycols with alcohols catalysed by Lewis acids, are absent or can be isolated as secondary products in very low yields. Zemplén deacetylation afforded the target glycosides in almost quantitative yields. Because the 6-deoxy glycol of the D series was not commercially available, we synthesized compounds **6–9** starting from the glycol 3,4,6-tri-*O*-acetyl-1,5-anhydro-2-deoxy-D-*arabino*-hex-1-enitol (**1**; Scheme 1). Tosylation at the primary position was easily accomplished with tosyl chloride in pyridine and dichloromethane at 0 °C in yields ranging from 84 to 93% for compounds **10–13**. The tosylation of only one OH group was confirmed by NMR spectroscopy due to the presence of characteristic doublets of the aromatic protons at  $\delta = 7.80$ – $7.33$  ppm and of the singlet at  $\delta = 2.43$ – $2.44$  ppm for the methyl group, which integrate for a single tosyl group in each compound. Moreover, the displacement of the chemical shifts of 6a-H and 6b-H to lower fields confirmed the selective substitution at 6-OH. Reduction of the tosylated compounds was first attempted with lithium triethylborohydride (super-hydride), but the single product obtained resulted from intramolecular cyclization as a result of S<sub>N</sub>2 displacement of the tosyloxy group by the 3-alkoxy group. The reduction of the tosyloxy group succeeded with lithium aluminium hydride in THF to afford the 2,6-dideoxy compounds **14–17** in yields of 70–79%, confirmed by the absence of signals corresponding to the tosyl group and the presence of chemical shifts for 6-CH<sub>3</sub> at  $\delta = 18.0$  ppm (carbon resonance). Although conventional, this is an efficient approach that leads to molecules with the 2,6-dideoxy pattern in a simple, high-yielding and reproducible manner. The 2,6-dideoxy L series glycosides **18–21** (Scheme 2) were synthesized starting from the commercially available 6-deoxy-L-glycol as described previously.<sup>[8]</sup>



Scheme 1. Synthesis of compounds 2–17. *Reagents and conditions:* i) 0.1 equiv. TPHB, 2 equiv. ROH, anhydrous CH<sub>2</sub>Cl<sub>2</sub>, room temp., 12 h; 69% for **2**, 15% for **3**, 83% for **4**, 12% for **5**; ii) a. MeONa, MeOH, pH 9, 45 min; b. Amberlite IR 120; 97% for **6**, 98% for **7**, 95% for **8**, 97% for **9**; c. 2 equiv. TsCl, CH<sub>2</sub>Cl<sub>2</sub>/Py (1:1), 0 °C to room temp., 2 h; 88% for **10**, 84% for **11**, 93% for **12**, 91% for **13**; iii) 3 equiv. LiAlH<sub>4</sub>, THF, 0 °C to room temp., 72 h; 70% for **14**, 72% for **15**, 79% for **16**, 75% for **17**.



Scheme 2. Structure of compounds **18–21** synthesized according to ref.<sup>[8]</sup>

### Surface Activity

The dependence of the surface tension,  $\gamma$ , on the molality,  $m$ , of the octyl and dodecyl 2,6-dideoxy- $\alpha$ -D-arabino-hexopyranosides (**14** and **16**, respectively) was evaluated. Measurements were also taken for the dodecyl 2,6-dideoxy- $\beta$ -D-arabino-hexopyranoside (**17**), but its very low solubility led to erroneous measurements for  $m \geq 1 \times 10^{-5}$  mol/kg. The data obtained from independent batches and dilutions of these compounds are in good agreement, which reconfirms the purity of the samples. Furthermore, no minimum near the CMC was observed in any of the plots (Figure 1), which indicates the absence of hydrophobic impurities in the synthesized and purified alkyl 2,6-dideoxy-D-arabino-hexopyranosides.<sup>[19]</sup>

Both plots show an identical pattern with three sections (Figure 1), two of them below the critical micelle concentration (CMC) and a third one above the CMC. In this last section the molality is almost independent of the surface tension. The presence of a break between the first two sections ( $47 < \gamma < 40$  mN/m) below the CMC indicates the formation of pre-micellar aggregates, a feature previously observed in our studies on alkyl 2-deoxy-D- and 2,6-dideoxy-L-arabino-hexopyranosides<sup>[8,9]</sup> as well as with commercial alkyl polyglucosides.<sup>[19–21]</sup>

The moduli of the pre-micellar slopes and surface excess obtained from the Gibbs plots (Figure 2) both increase with alkyl chain length, as expected from the increased hydrophobicity of the compounds. Post-micellar slopes for the octyl derivative **14** are more negative than those of the do-

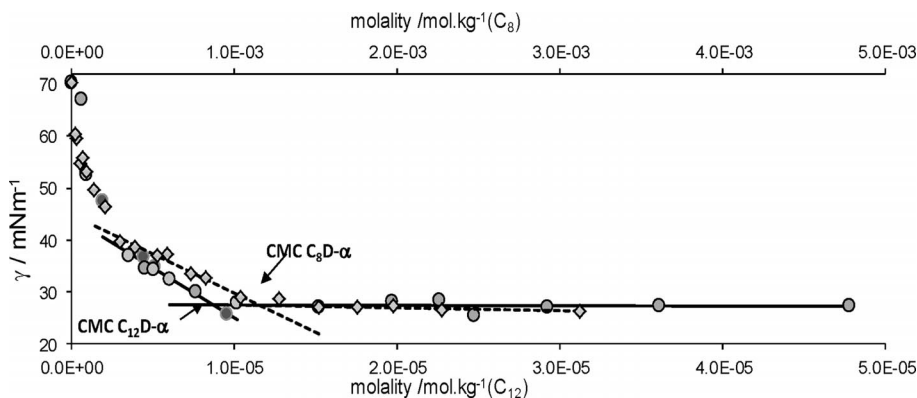


Figure 1. Dependence of surface tension on the concentration of aqueous solutions of octyl 2,6-dideoxy- $\alpha$ -D-arabino-hexopyranoside (**14**) and dodecyl 2,6-dideoxy- $\alpha$ -D-arabino-hexopyranoside (**16**) at 35 °C.

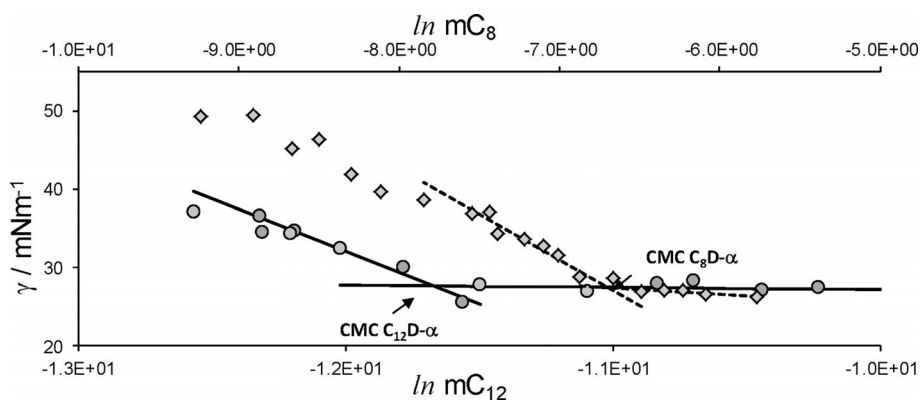


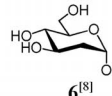
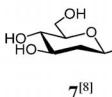
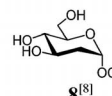
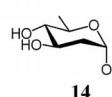
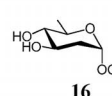
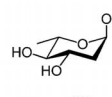
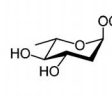
Figure 2. Gibbs plots for aqueous solutions of octyl 2,6-dideoxy- $\alpha$ -D-arabino-hexopyranoside (**14**) and dodecyl 2,6-dideoxy- $\alpha$ -D-arabino-hexopyranoside (**16**) at 35 °C.

decyl derivative, which suggests a less efficient packing at the air/water interface and indicates the formation of micellar aggregates with an increased degree of polydispersity.

The surface activity parameters for compounds **14** and **16** were compared with the corresponding data for their enantiomers **18** and **20**, respectively, as well as with data previously obtained for the 2-deoxy glycosides. Compounds **19** and **21** presented a very low solubility, as observed for compound **17**, and were not tested. The data previously published<sup>[8,9]</sup> were refined with a new set of data obtained for new batches of **18** and **20**, evaluated with an automatic tensiometer instead of the manual Kruss K8 previously used. Recalculated values for these enantiomers over a larger concentration range are summarized in Table 1. The results demonstrate that deoxygenation of the glycoside head-groups promotes aggregation, leading to a decrease in the CMC and an increase in the adsorption efficiency ( $pC_{20}$ ). Therefore the  $CMC/C_{20}$  ratio was calculated to screen for the role of structural microenvironmental factors on both these parameters. The ratio decreases with chain length for 2-deoxy- and 2,6-dideoxy glycopyranosides of the L and D series, which indicates that increasing the alkyl chain promotes aggregation more efficiently than adsorption. The  $CMC/C_{20}$  ratio decreases more abruptly for the D series dideoxy derivatives than for 2-deoxy glycosides, which suggests that removal of the hydroxy group at the 6-position is crucial to increase aggregation.

The remarkable difference in the magnifying ratio  $CMC/C_{20}$  of the octyl dideoxy glycosides may result from the polydisperse nature of these aggregates. A longer alkyl chain promotes stronger attractive chain interactions and facilitates molecular aggregation. Although the measured CMC for dodecyl dideoxy  $\alpha$ -D-glycoside is lower than that of its enantiomer, the surface excesses are virtually identical within their uncertainties. This unexpected behaviour was verified with different batches of the L enantiomer **20**. The decrease observed in the  $CMC/C_{20}$  ratio on going from octyl to dodecyl dideoxy glycosides of the L series is less than that for their enantiomeric glycosides. This suggests a better packing efficiency for the former dideoxy glycosides than for the dideoxy-D-glycopyranosides. However, these differ-

Table 1. Adsorption properties of alkyl deoxy glycosides at the air/water interface.<sup>[a]</sup>

Compound	$CMC$ /mol kg <sup>-1</sup>	$pC_{20}$	$CMC$ / $C_{20}$	$\Gamma_2 \times 10^6$ /mol m <sup>-2</sup>	$a_m \times 10^{20}$ /m <sup>2</sup>
 <b>6</b> <sup>[8]</sup>	$2.2 \times 10^{-3}$ $\pm 0.1 \times 10^{-3}$	3.3 $\pm 0.1$	4.6 $\pm 0.1$	4.2 $\pm 0.1$	39 $\pm 1$
 <b>7</b> <sup>[8]</sup>	$2.2 \times 10^{-3}$ $\pm 0.1 \times 10^{-3}$	3.3 $\pm 0.1$	5.0 $\pm 0.9$	4.1 $\pm 0.1$	41 $\pm 1$
 <b>8</b> <sup>[8]</sup>	$2.54 \times 10^{-5}$ $\pm 0.01 \times 10^{-5}$	5.1 $\pm 0.1$	3.3 $\pm 0.4$	5.0 $\pm 1.0$	33 $\pm 2$
 <b>14</b>	$1.24 \times 10^{-3}$ $\pm 0.02 \times 10^{-3}$	4.0 $\pm 0.1$	13.5 $\pm 2.0$	4.6 $\pm 0.5$	36 $\pm 4$
 <b>16</b>	$0.86 \times 10^{-5}$ $\pm 0.02 \times 10^{-5}$	5.7 $\pm 0.3$	4.3 $\pm 2.0$	5.2 $\pm 0.4$	32 $\pm 2$
 <b>18</b>	$1.10 \times 10^{-3}$ $\pm 0.05 \times 10^{-3}$	3.8 $\pm 0.1$	6.5 $\pm 2.0$	4.0 $\pm 0.2$	41 $\pm 2$
 <b>20</b>	$1.21 \times 10^{-5}$ $\pm 0.02 \times 10^{-5}$	5.7 $\pm 0.1$	4.6 $\pm 0.7$	5.6 $\pm 0.6$	30 $\pm 3$

[a]  $a_m$ : molecular area on a saturated liquid/air interface.

ences are within the  $CMC/C_{20}$  uncertainties of the dodecyl glycosides.

The removal of the hydroxy group from the 6-position generates other remarkable changes in the physical (thermotropic) properties and an inversion in the solubility. Deoxygenation at only the 2-position leads to direct transitions from the solid crystalline state to the isotropic liquid melts

and to a decrease in the melting points, as observed for the octyl and dodecyl 2-deoxy-D-*arabino*-hexopyranosides previously studied<sup>[8]</sup> (Table 2). Nevertheless, the solubility pattern of D-glucosides is retained, namely the  $\beta$  anomers are more soluble than the corresponding  $\alpha$  anomers.<sup>[8,19,20]</sup> However, upon additional deoxygenation at the 6-position, a small decrease in the melting point of both  $\beta$  anomers and an abrupt decrease for both  $\alpha$  anomers is observed and, concurrently, an inversion in the solubility pattern is also detected.

Table 2. Transition temperatures of alkyl glucosides to isotropic liquids.

Compound	Transition temp. [°C]	
	$\alpha$ anomer	$\beta$ anomer
Octyl 2,6-dideoxy-D- <i>arabino</i> -hexopyranoside	<25	80
Dodecyl 2,6-dideoxy-D- <i>arabino</i> -hexopyranoside	36	97
Octyl 2,6-dideoxy-L- <i>arabino</i> -hexopyranoside	<25	68 <sup>[9]</sup>
Dodecyl 2,6-dideoxy-L- <i>arabino</i> -hexopyranoside	36	82 <sup>[9]</sup>
Octyl 2-deoxy-D- <i>arabino</i> -hexopyranoside	107 <sup>[8]</sup>	85.5 <sup>[8]</sup>
Dodecyl 2-deoxy-D- <i>arabino</i> -hexopyranoside	114.8 <sup>[8]</sup>	102.3 <sup>[8]</sup>
Octyl D-glucopyranoside	115 <sup>[22]</sup>	104.5 <sup>[22]</sup> , 99 <sup>[23]</sup>
Decyl D-glucopyranoside	136 <sup>[22]</sup>	140 <sup>[22]</sup> , 137 <sup>[23]</sup>
Dodecyl D-glucopyranoside	148 <sup>[22]</sup>	146 <sup>[22]</sup>

These findings suggest that the thermotropic behaviour is dictated by intermolecular hydrogen bonding of the head-group and tuned by hydrophobic interactions in both glucopyranosides<sup>[22,23]</sup> and 2-deoxy-*arabino*-hexopyranosides.<sup>[8]</sup> Further deoxygenation at the 6-position significantly reduces the hydrogen bonding and the melting point and solubility become processes ruled by hydrophobic interactions.<sup>[24]</sup>

The apparent inconsistency in the previously reported melting point of **20** (34 °C)<sup>[9]</sup> was verified by evaluating the melting point of the newly synthesized compound. A dried sample of **20** revealed time-dependent melting points ranging from 36.2 to 41.6 °C, which may indicate the presence of concomitant polymorphs.<sup>[25]</sup>

## Antibacterial Activity

The synthesized compounds were evaluated for their antimicrobial activity first by the paper disk diffusion method. The results are expressed as the average diameter of the inhibition zone detected in three replicates (Table 3).

The minimal inhibitory concentrations (MIC) were determined for those compounds that showed considerable activity in the preliminary paper disk assays and the results are presented in Table 3. The dodecyl  $\alpha$ -D-glycoside **16** shows the highest diameter of inhibition towards *Bacillus cereus* of all the compounds tested, even higher than that of the reference antibiotic chloramphenicol at the same concentration. This compound also promoted significant growth inhibition of *Bacillus subtilis*, *Enterococcus faecalis* and *Listeria monocytogenes*, with inhibition diameters varying from 17  $\pm$  7 to 28  $\pm$  12 mm. Its stereoisomer with all the stereogenic centres bearing an inverted configuration, the dodecyl  $\alpha$ -L-glycoside **20**, also showed significant activity towards the *Bacillus* species, particularly *B. cereus*. However, the  $\beta$  anomers **17** and **21** were completely inactive, which suggests that the anomeric configuration plays an important role in the antimicrobial activity towards the *Bacillus* species.

In spite of the low solubility of the  $\alpha$ -D-glycoside **16**, the local concentration on the *Bacillus* membrane may be significant in view of the high value of pC<sub>20</sub> determined for this compound. The presence of the dodecyl chain is also determinant of the bioactivity exhibited by the 2,6-dideoxy glycosides of both the D and L series.

None of the synthesized compounds at the tested concentrations revealed significant activity towards *Salmonella enteritidis*, *Pseudomonas aeruginosa* or *Escherichia coli*. However, the dodecyl 2-deoxy- $\beta$ -D-glycoside **9** showed significant activity towards *Enterococcus faecalis*. The  $\alpha$  anomers **6** and **8** were inactive towards all the microbes tested.<sup>[8]</sup>

The antibacterial activities of this new family of antibiotics towards *B. anthracis* are reported for the first time. The MICs of the most active compounds towards *B. anthracis*, *B. cereus*, *B. subtilis*, *E. faecalis* and *L. monocytogenes* are presented in Table 4. The dodecyl  $\alpha$ -L-glycoside **20** was the

Table 3. Antibacterial activities expressed as the diameter of the inhibition zones ( $\pm$  standard deviation) for compounds **7**, **9**, **14–16** and **18–20** and comparison with the activities of the control (chloramphenicol) using the paper disc diffusion method.<sup>[a,b]</sup>

Bacteria	Diameter of inhibition [mm]									
	<b>7</b> <sup>[8]</sup>	<b>9</b> <sup>[8]</sup>	<b>14</b>	<b>15</b>	<b>16</b>	<b>18</b> <sup>[8]</sup>	<b>19</b> <sup>[8]</sup>	<b>20</b> <sup>[8]</sup>	Control <sup>[c]</sup>	
									I	II
<i>B. cereus</i>	11 $\pm$ 1	10 $\pm$ 0	13 $\pm$ 3	11 $\pm$ 3	58 $\pm$ 16	12 $\pm$ 2	12 $\pm$ 2	27 $\pm$ 5	25 $\pm$ 3	40 $\pm$ 5
<i>B. subtilis</i>	12 $\pm$ 1	10 $\pm$ 0	14 $\pm$ 1	13 $\pm$ 1	28 $\pm$ 12	12 $\pm$ 2	10 $\pm$ 0	25 $\pm$ 3	30 $\pm$ 3	46 $\pm$ 3
<i>E. faecalis</i>	14 $\pm$ 0	17 $\pm$ 2	11 $\pm$ 1	9 $\pm$ 0	23 $\pm$ 12	10 $\pm$ 0	9 $\pm$ 2	13 $\pm$ 2	29 $\pm$ 4	39 $\pm$ 4
<i>E. coli</i>	<6.4	<6.4	8 $\pm$ 0	<6.4	<6.4	8 $\pm$ 1	9 $\pm$ 0	<6.4	29 $\pm$ 3	42 $\pm$ 4
<i>L. monocytogenes</i>	<6.4	<6.4	10 $\pm$ 1	9 $\pm$ 1	17 $\pm$ 7	10 $\pm$ 1	10 $\pm$ 1	12 $\pm$ 2	32 $\pm$ 4	45 $\pm$ 3
<i>P. aeruginosa</i>	<6.4	<6.4	10 $\pm$ 1	9 $\pm$ 1	<6.4	8 $\pm$ 0	9 $\pm$ 0	<6.4	<6.4	22 $\pm$ 2
<i>S. enteritidis</i>	<6.4	<6.4	8 $\pm$ 1	9 $\pm$ 1	<6.4	<6.4	<6.4	<6.4	30 $\pm$ 3	42 $\pm$ 3
<i>S. aureus</i>	<6.4	<6.4	12 $\pm$ 1	10 $\pm$ 1	8 $\pm$ 0	11 $\pm$ 1	12 $\pm$ 3	9 $\pm$ 1	27 $\pm$ 5	42 $\pm$ 6

[a] A solution of the compound (300  $\mu$ g) in DMSO (15  $\mu$ L) was applied on the disk. [b] The inhibition diameter was <6.4 mm for all the bacteria tested for compounds **6**,<sup>[8]</sup> **17** and **21**.<sup>[8]</sup> Compound **8** was also considered inactive (inhibition diameters of 9 and 10 mm for *B. subtilis* and *L. monocytogenes*).<sup>[8]</sup> [c] Solutions of chloramphenicol in DMSO (15  $\mu$ L) were used as controls (I: 30  $\mu$ g; II: 300  $\mu$ g).

most effective compound tested, showing a MIC value of 25  $\mu\text{M}$  with *Bacillus* spp., followed by its enantiomer **16**. The  $\beta$ -glycosides **7** and **9** were ineffective against the *Bacillus* species, presenting a MIC of only 112 and 93  $\mu\text{M}$ , respectively, with *E. faecalis*.

Table 4. Antibacterial activities expressed as MIC for compounds **7**, **9**, **16** and **20** in comparison with the activities of the control (chloramphenicol).<sup>[a]</sup>

Bacteria	MIC [mM]				Control
	<b>7</b>	<b>9</b>	<b>16</b>	<b>20</b>	
<i>B. anthracis</i> (pathogenic)	n.d.	>0.770	0.050	0.025	0.025
<i>B. anthracis</i> (vacinal)	n.d.	>0.770	0.050	0.025	0.025
<i>B. anthracis</i> (ovine)	n.d.	>0.770	0.050	0.025	0.025
<i>B. cereus</i>	>1.809 <sup>[8]</sup>	>1.504 <sup>[8]</sup>	0.025	0.025 <sup>[8]</sup>	0.019
<i>B. subtilis</i>	>1.809 <sup>[8]</sup>	>1.504 <sup>[8]</sup>	0.050	0.025 <sup>[8]</sup>	0.009
<i>E. faecalis</i>	0.112 <sup>[8]</sup>	0.093 <sup>[8]</sup>	0.050	0.050 <sup>[8]</sup>	0.019
<i>L. monocytogenes</i>	n.d.	0.752 <sup>[8]</sup>	0.050	0.100 <sup>[8]</sup>	0.019

[a] MICs for the *B. anthracis* strains were determined by the agar dilution method (concentrations ranging from 1–256  $\mu\text{g}/\text{mL}$ ), whereas the MICs for the remaining bacteria were evaluated by the broth dilution method (concentrations ranging from 1–500  $\mu\text{g}/\text{mL}$ ).

The mechanism of action of the synthesized alkyl glycosides is not clear, but preliminary work performed by our group on *B. cereus* suggests that these compounds may interact with the cellular membrane, altering its permeability and causing autolysis followed by cell death.<sup>[13]</sup> This hypothesis is supported by the surface activity results. The CMC of dodecyl 2,6-dideoxy- $\alpha$ -D-arabino-hexopyranoside (**16**) is the lowest observed (Table 1) whereas dodecyl 2,6-dideoxy- $\alpha$ -L-arabino-hexopyranoside (**20**) presents the highest surface excess. The latter parameter is indicative of a higher adsorption tendency at interfaces, which indicates that slightly higher drug concentrations on the *Bacillus* membrane will be found. This minor difference between these parameters for the two enantiomers, if not lying within the uncertainties, could account for the higher MIC obtained for **16** (16  $\mu\text{g}/\text{mL}$ , 50  $\mu\text{M}$ ) compared with that of its L enantiomer **20** (8  $\mu\text{g}/\text{mL}$ , 25  $\mu\text{M}$ ).

### Anticholinesterase Activity

The AChE and BChE inhibitory activities of some of the synthesized alkyl glycosides and those of the standards, rivastigmine and donepezil, two drugs used to treat Alzheimer's disease, are now discussed. None of the tested compounds significantly inhibited AChE, but at a concentration of 100  $\mu\text{g}/\text{mL}$ , the octyl 2-deoxy- $\alpha$ -D-glycoside **6** caused 100% inhibition of BChE and compound **8**, its dodecyl  $\alpha$ -D homologue, caused 81% inhibition at the same concentration. The final concentration of the tested compounds was ten-fold higher than that of the non-selective BChE inhibitors rivastigmine and donepezil, which showed 100 and 75% inhibition, respectively, of BChE. However, the structures of these glycoside inhibitors seem to be quite promis-

ing as scaffolds for future developments because no commercial drugs are available that selectively inhibit BChE. To assess the type of inhibition of compound **6**, the kinetic parameters  $K_m'$  and  $V'$  (apparent  $K_m$  and  $V$ , respectively) were determined for increasing inhibitor concentrations.  $V'$  did not show any significant change, whereas the values of  $K_m'$  increased. These results suggest that this compound is a competitive inhibitor of BChE and the competitive inhibitor constant  $K_i = 0.36$  mM was calculated from the intercept of the straight line with the inhibitor axis plotted in Figure 3. None of the alkyl 2,6-dideoxy glycosides tested, nor the compounds belonging to the 2-deoxy- $\beta$ -D series, revealed significant inhibitory activity towards BChE.

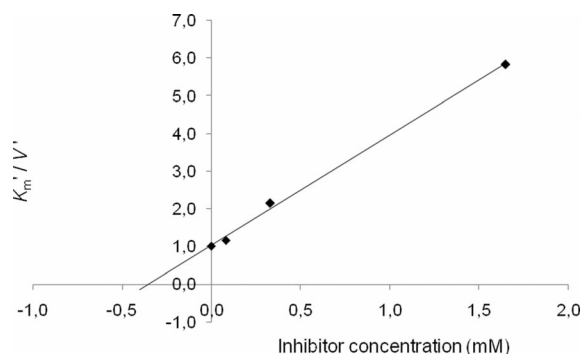


Figure 3. Plot of  $K_m'/V'$  versus concentration of octyl 2-deoxy- $\alpha$ -D-glycoside **6** ( $K_m'$  is the apparent  $K_m$  and  $V'$  is the apparent  $V$ ). The intercept of the resulting straight line with inhibitor axis gives a value of  $-K_i$ .

### Molecular Docking Studies

The molecular docking calculations of the most active glycoside **6**, its  $\beta$  anomer **7** and the corresponding 2,6-dideoxy compounds **14** and **15** were performed with BChE to rationalize the selectivity observed for compound **6**. Even though the interaction energies are similar (ca.  $-7$  kcal/mol), we observed very different modes of binding. Our cluster analysis generated up to 250 conformational clusters and we visually analysed the most abundant. These were grouped by their specific mode of binding to the different residues in the active site. Indeed, ligand **6** presented a lowest-energy conformation with several interactions with the two accessible residues of the catalytic triad, namely Ser-198 and His-438 (see Figure 4, a). The high abundance of this mode of binding was confirmed by the cluster analysis of the conformational data obtained (ca. 61% of the solutions show a direct interaction with the catalytic residues).

Interestingly, it is the most flexible hydroxy group (bound to C-6) that is placed at a hydrogen-bonding distance to both catalytic residues, stabilizing the protein-inhibitor complex. Even though the active site cavity is significantly large in BChE, a complex of this type completely blocks the substrate access to the catalytic triad. Ligand **7** is the  $\beta$  stereoisomer of **6** and its binding mode changes with this geometric constraint (Figure 4, b). With this change in anomeric orientation, the ligand moves away from His-438

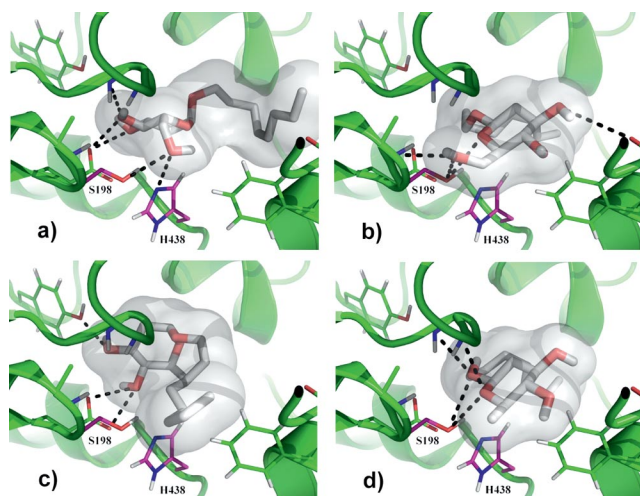


Figure 4. Lowest-energy solutions from the docking calculations of the deoxy glycoside ligands (grey) **6** (a), **7** (b), **14** (c) and **15** (d) in BChE (green). Interactions are represented by black dashed lines. The catalytic residues are shown with the carbon atoms represented in pink.

while maintaining a direct interaction with Ser-198. This interaction remains the most abundant (ca. 54%).

Glycoside **14** differs from **6** as it bears a second deoxy position at C-6, and this has a significant impact on its binding mode to BChE (Figure 4, c). Removal of this key OH group induces a strong slide of the ligand away from the catalytic triad, which results in the absence of interactions with any of these residues in many conformational clusters. The  $\beta$  stereoisomer of **14** is ligand **15**, which seems to bind to BChE similarly to the previous  $\beta$  ligand **7**. In the absence of the OH group at the 6-position, this ligand adopts a conformation that favours the interaction with Ser-198 through the endocyclic oxygen (Figure 4, d). Unlike glycoside **14**, the interaction of compound **15** with Ser-198 renders a low-energy conformational cluster, which contributes significantly to its predominant mode of binding (ca. 50%).

These results show significant differences in the modes of binding of the glycosides studied, with compound **6** presenting the most promising interactions. In fact, this ligand displays a network of hydrogen bonds with all the accessible residues of the catalytic triad, which may explain the higher inhibition determined experimentally. Although compound **6** displayed significant inhibition of BChE, it was not effective in the assays with AChE. To rationalize these experimental results, similar docking studies of **6** on AChE were performed. However, the observed binding modes were not significantly different to account for the contrasting inhibition profiles obtained. These puzzling results prompted us to analyse in detail the access to the active site cavities of BChE and AChE.

Figure 5 illustrates the differences between the two X-ray structures.<sup>[26,27]</sup> The catalytic triad structure is conserved, but there are major differences in the size and shape of the active site entrance. AChE exhibits several bulky residues that hinder access to the active site cavity. Even though

these observations are based on rigid crystal structures, there is significant evidence that the selective inhibition of BChE by compound **6** is a result of this size-exclusion mechanism.

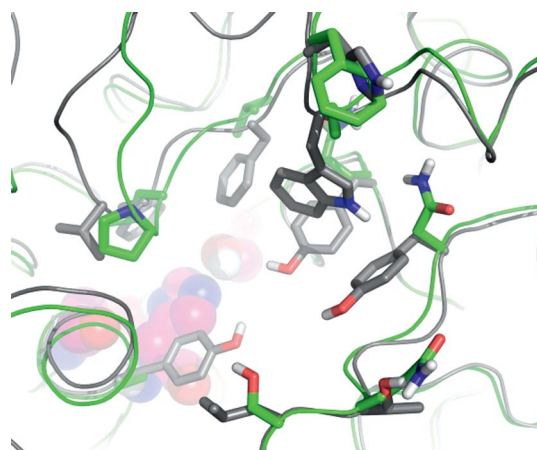


Figure 5. Structural representation of the amino acids around the active site cavity that differ in the protein sequences of both BChE (green)<sup>[26]</sup> and AChE (grey).<sup>[27]</sup> The main chains of the proteins are shown as ribbons. The catalytic residues are shown as spheres with the carbon atoms represented in pink.

Figure 6 shows the lowest-energy solutions of the first 10 clusters obtained in the docking calculations of compound **6** in BChE and AChE. The docking solutions of BChE concentrate on the catalytic residues in a cavity that is large enough for the inhibitor to adopt its preferred conformation and form stable enzyme–inhibitor complexes. Access to the AChE active site is partially occluded resulting in a significant amount of the docking clusters outside the cavity of interest. The difficulty in generating docking solutions closer to the catalytic triad together with the narrow entrance to the active site can generate a kinetic barrier for these compounds to access their target. Such a barrier will have an impact on the activity/inhibition profiles of the enzyme and may explain the inhibition results obtained for deoxy glycoside **6** with AChE.

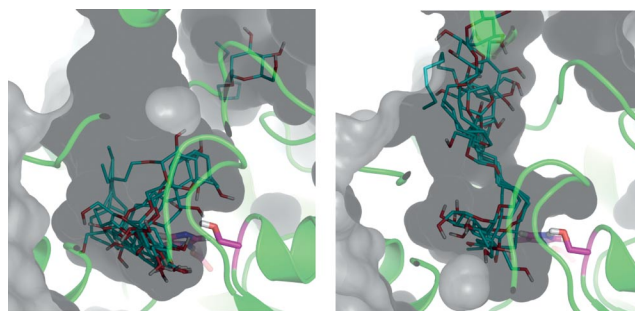


Figure 6. Lowest-energy solutions for the first 10 clusters obtained in the docking calculations of compound **6** (cyan) in BChE (left) and AChE (right). The protein surface is shown in grey to illustrate the active site cavity. The catalytic residues are shown with carbon atoms represented in pink.



## Conclusions

Alkyl 2-deoxy- and 2,6-dideoxy-*arabino*-hexopyranosides have been explored from a multidisciplinary perspective. Organic and physical chemistry techniques were used to produce new molecules and correlate their properties with their biological behaviour.

To estimate the most important physical phenomena that contribute to the antimicrobial activities exhibited by this new family of antibiotics, parameters related to molecule aggregation and adsorption at the air/water interface were evaluated. It was found that removal of the hydroxy group at the 6-position is crucial to increasing aggregation over adsorption. The decrease observed in the CMC/C<sub>20</sub> ratio on going from octyl to dodecyl dideoxy glycosides suggests a better packing efficiency of the L series glycosides. However, these results are within experimental uncertainties. The  $\alpha$ -anomeric configuration and the 2,6-dideoxygenation pattern proved to be essential for antibacterial activity against the *Bacillus* species tested. The L configuration enhanced this activity, particularly towards *Bacillus anthracis*.

On the other hand, the presence of the primary hydroxy group at C-6 was found to be crucial for the inhibition of BChE by octyl 2-deoxy- $\alpha$ -D-glycoside **6** and its dodecyl  $\alpha$ -D homologue **8**. The inhibition type was assessed for the most active glycoside **6** and it was found to be competitive. Docking studies have helped us to understand the role of the flexible hydroxy group in the active site and to rationalize the lack of activity of the  $\beta$  anomers as well as that of the corresponding dideoxy  $\alpha$  anomers. The observed selectivity towards BChE was unexpected due to the similarities between the BChE and AChE active sites. However, it could be explained by the physical hindrances experienced by the inhibitor when accessing the active site of AChE.

This work highlights the importance of organic chemistry in tuning alkyl glycoside bioactivity through structural features such as the D or L configuration, the deoxygenation pattern and the orientation of the anomeric substituent. Furthermore, the adopted methodology for the synthesis of the studied deoxy glycosides has the advantage of delivering the  $\alpha$  anomer as the major reaction product, which show the greatest bioactivity. In addition, new leads have been reported that encourage further study of these molecular entities aiming at the development of new drug candidates with new mechanisms of action to overcome antibiotic resistance and/or neurodegenerative impairments, two major concerns in today's society.

## Experimental Section

**General:** Starting materials and reagents were purchased from Sigma–Aldrich, Fluka and Acros. The solvents were dried prior to use with 4 or 3 Å (methanol) molecular sieves. Compounds **2–9** were synthesized according to the procedures previously described by us.<sup>[8]</sup> The spectroscopic and physical data of these compounds are in agreement with those previously reported, with the exception of the specific rotation of compound **7**, which is corrected to  $\alpha_D^{20} = -1.3$  ( $c = 1$ , CH<sub>2</sub>Cl<sub>2</sub>).

TLC was carried out on aluminium sheets (20 cm × 20 cm) coated with 0.2 mm silica gel 60 F-254 (Merck) and detection was accomplished by spraying the plates with a solution of H<sub>2</sub>SO<sub>4</sub> in ethanol (10%) followed by heating at 120 °C.

The compounds were purified by column chromatography (CC) using silica gel 60G (0.040–0.063 mm, Merck) or silica gel 60G (0.015–0.040 mm, Merck)

Melting points were first obtained with an SMP3 Melting Point Apparatus, Stuart Scientific, Bibby. Elemental analyses were performed by the Microanalysis Service of the Instituto Superior Técnico, Universidade Técnica de Lisboa. Optical rotations were measured with a Perkin–Elmer 343 polarimeter.

NMR spectra were recorded with a Bruker Avance 400 spectrometer at 298 K operating at 100.62 MHz for <sup>13</sup>C NMR and at 400.13 MHz for <sup>1</sup>H NMR. The solvents used were CDCl<sub>3</sub> with 0.03% TMS and CD<sub>3</sub>OD (Sigma–Aldrich). The chemical shifts are reported as  $\delta$  (ppm) and the coupling constants ( $J$ ) are given in Hz.

**General Procedure for the Tosylation Reaction:** TsCl (3.3 mmol) and pyridine (3 mL) were added to a solution of the alkyl 2-deoxy-D-*arabino*-hexopyranoside (1.5 mmol) in CH<sub>2</sub>Cl<sub>2</sub> (3 mL) at 0 °C and the reaction mixture was stirred at room temp. for 2 h. The solution was washed with a satd. solution of NaHCO<sub>3</sub> and the organic phase was washed with water and dried with sodium sulfate. After filtration, the organic phase was evaporated in the rotavapor to give a residue that was purified by CC eluting with EtOAc/cyclohexane (1:1) to afford the product.

**Octyl 2-Deoxy-6-O-tosyl- $\alpha$ -D-*arabino*-hexopyranoside (**10**):** The above-mentioned procedure gave **10** as a syrup (0.57 g, 88.0%).  $\alpha_D^{20} = +2.2$  ( $c = 1$ , CH<sub>2</sub>Cl<sub>2</sub>).  $R_f = 0.49$  (1:1 EtOAc/cyclohexane). <sup>1</sup>H NMR (400 MHz, CDCl<sub>3</sub>):  $\delta = 7.80$  (d, 2 H, Ph-Ts), 7.34 (d, 2 H, Ph-Ts), 4.80 (d, <sup>3</sup> $J_{1,2a} = 2.78$  Hz, 1 H, 1-H), 4.36 (dd, <sup>2</sup> $J_{6a,6b} = 10.86$ , <sup>3</sup> $J_{6a,5} = 4.55$  Hz, 1 H, 6a-H), 4.24 (dd, <sup>3</sup> $J_{6b,5} = 1.01$ , <sup>2</sup> $J_{6a,6b} = 10.86$  Hz, 1 H, 6b-H), 3.92 (ddd, <sup>3</sup> $J_{3,2a} = 9.6$ , <sup>3</sup> $J_{3,2e} = 5.00$ , <sup>3</sup> $J_{4,3} = 9.1$  Hz, 1 H, 3-H), 3.69 (ddd, <sup>3</sup> $J_{5,6b} = 1.01$ , <sup>3</sup> $J_{5,6a} = 4.30$ , <sup>3</sup> $J_{4,5} = 9.1$  Hz, 1 H, 5-H), 3.51 (ddd, <sup>2</sup> $J_{1'a,1'b} = 9.6$ , <sup>3</sup> $J_{1'a,2'a} = 3.1$ , <sup>3</sup> $J_{1'a,2'b} = 6.95$  Hz, 1 H, 1'a-H), 3.38 (t, <sup>3</sup> $J_{4,3} = 3.4$ , <sup>3</sup> $J_{4,5} = 9.1$  Hz, 1 H, 4-H), 3.23 (ddd, <sup>3</sup> $J_{1'b,2'b} = 3.1$ , <sup>2</sup> $J_{1'b,2'a} = 6.82$ , <sup>2</sup> $J_{1'a,1'b} = 9.6$  Hz, 1 H, 1'b-H), 2.43 (s, 3 H CH<sub>3</sub>-Ts), 2.08 (dd, <sup>2</sup> $J_{2e,2a} = 12.88$ , <sup>3</sup> $J_{2e,3} = 4.8$  Hz, 1 H, 2e-H), 1.62 (td, <sup>2</sup> $J_{2a,3} = 9.6$ , <sup>2</sup> $J_{2e,2a} = 12.88$  Hz, 1 H, 2a-H), 1.52–1.48 (m, 2-H, 2'a-H, 2'b-H), 1.31–1.23 (m, 10 H, 3'a,b-H to 7'a,b-H), 0.88 (t, <sup>3</sup> $J_{7',8'} = 6.82$  Hz, 3 H, 8'-H) ppm. <sup>13</sup>C NMR (100.62 MHz, CDCl<sub>3</sub>):  $\delta = 144.5$ , 132.7, 129.8, 127.9 (Ph-Ts), 101.9 (C-1), 78.8 (C-4), 73.9 (C-5), 73.3 (C-3), 71.1 (C-1'), 63.7 (C-6), 41.2 (C-2), 33.8, 31.5, 31.3, 31.2, 27.9, 24.5 (C-2' to C-7'), 15.2 (C-8') ppm. C<sub>21</sub>H<sub>34</sub>O<sub>7</sub>S (430.20): calcd. C 58.58, H 7.97; found C 58.55, H 7.95.

**Octyl 2-Deoxy-6-O-tosyl- $\beta$ -D-*arabino*-hexopyranoside (**11**):** The above-mentioned procedure gave **11** as a syrup (0.54 g, 84.3%).  $\alpha_D^{20} = -5.1$  ( $c = 1$ , CH<sub>2</sub>Cl<sub>2</sub>).  $R_f = 0.45$  (1:1 EtOAc/cyclohexane). <sup>1</sup>H NMR (400 MHz, CDCl<sub>3</sub>):  $\delta = 7.80$  (d, 2 H, Ph-Ts), 7.34 (d, 2 H, Ph-Ts), 4.47 (d, <sup>3</sup> $J_{1,2a} = 8.08$  Hz, 1 H, 1-H), 4.36 (dd, <sup>2</sup> $J_{6a,6b} = 10.86$ , <sup>3</sup> $J_{6a,5} = 4.55$  Hz, 1 H, 6a-H), 4.24 (dd, <sup>3</sup> $J_{6b,5} = 1.01$ , <sup>2</sup> $J_{6a,6b} = 10.86$  Hz, 1 H, 6b-H), 3.76 (ddd, <sup>3</sup> $J_{1'a,2'b} = 3.1$ , <sup>3</sup> $J_{1'a,2'a} = 6.69$ , <sup>2</sup> $J_{1'a,1'b} = 9.35$  Hz, 1 H, 1'a-H), 3.64 (ddd, <sup>3</sup> $J_{3,4} = 9.1$ , <sup>3</sup> $J_{3,2a} = 9.6$ , <sup>3</sup> $J_{3,2e} = 4.8$  Hz, 1 H, 3-H), 3.40–3.34 (m, 3 H, 4-H, 5-H, 1'b-H), 2.43 (s, 3 H, CH<sub>3</sub>-Ts), 2.08 (dd, <sup>2</sup> $J_{2e,2a} = 12.88$ , <sup>3</sup> $J_{2e,3} = 4.8$  Hz, 1 H, 2e-H), 1.62 (td, <sup>3</sup> $J_{2a,3} = 9.6$ , <sup>2</sup> $J_{2e,2a} = 12.88$  Hz, 1 H, 2a-H), 1.52–1.48 (m, 2 H, 2'b-H), 1.31–1.23 (m, 10 H, 3'a,b-H to 7'a,b-H), 0.88 (t, <sup>3</sup> $J_{7',8'} = 6.82$  Hz, 3 H, 8'-H) ppm. <sup>13</sup>C NMR (100.62 MHz, CDCl<sub>3</sub>):  $\delta = 144.5$ , 132.7, 129.8, 127.9 (Ph-Ts), 101.9 (C-1), 78.8 (C-5), 73.9 (C-4), 73.3 (C-3), 69.6 (C-1'), 69.0 (C-6), 41.2 (C-2), 33.8, 31.5, 31.3, 31.2, 27.9, 24.5 (C-2' to C-7'), 15.2 (C-8') ppm. C<sub>21</sub>H<sub>34</sub>O<sub>7</sub>S (430.20): calcd. C 58.58, H 7.97; found C 58.57, H 7.93.

**Dodecyl 2-Deoxy-6-O-tosyl- $\alpha$ -D-arabino-hexopyranoside (12):** The above-mentioned procedure gave **12** as a syrup (0.68 g, 92.9%).  $\alpha_D^{20} = +2.4$  ( $c = 1$ ,  $\text{CH}_2\text{Cl}_2$ ).  $R_f = 0.53$  (1:1 EtOAc/cyclohexane).  $^1\text{H}$  NMR (400 MHz,  $\text{CDCl}_3$ ):  $\delta = 7.82$  (d, 2 H, Ph-Ts), 7.33 (d, 2 H, Ph-Ts), 4.81 (d,  $^3J_{1,2a} = 2.27$  Hz, 1 H, 1-H), 4.40 (dd,  $^2J_{6a,6b} = 10.86$ ,  $^3J_{6a,5} = 4.30$  Hz, 1 H, 6a-H), 4.21 (dd,  $^3J_{6b,5} = 1.01$ ,  $^2J_{6a,6b} = 10.86$  Hz, 1 H, 6b-H), 3.95 (ddd,  $^3J_{3,2a} = 9.6$ ,  $^3J_{3,2e} = 5.05$ ,  $^3J_{4,3} = 9.1$  Hz, 1 H, 3-H), 3.69 (ddd,  $^3J_{5,6b} = 1.01$ ,  $^3J_{5,6a} = 4.30$ ,  $^3J_{4,5} = 9.1$  Hz, 1 H, 5-H), 3.52 (ddd,  $^2J_{1'a,1'b} = 9.6$ ,  $^3J_{1'a,2'a} = ^3J_{1'a,2'b} = 6.95$  Hz, 1 H, 1'a-H), 3.42 (t,  $^3J_{4,3} = ^3J_{4,5} = 9.1$  Hz, 1 H, 4-H), 3.28 (ddd,  $^3J_{1'b,2'b} = ^3J_{1'b,2'a} = 6.82$ ,  $^2J_{1'a,1'b} = 9.6$  Hz, 1 H, 1'b-H), 2.44 (s, 3 H,  $\text{CH}_3$ -Ts), 2.10 (dd,  $^2J_{2e,2a} = 12.88$ ,  $^3J_{2e,3} = 5.05$  Hz, 1 H, 2e-H), 1.64 (td,  $^3J_{2a,3} = 9.6$ ,  $^2J_{2e,2a} = 12.88$  Hz, 1 H, 2a-H), 1.51–1.48 (m, 2 H, 2'a-H, 2'b-H), 1.32–1.22 (m, 18 H, 3'a,b-H to 11'a,b-H), 0.88 (t,  $^3J_{11',12'} = 6.32$  Hz, 3 H, 12'-H) ppm.  $^{13}\text{C}$  NMR (100.62 MHz,  $\text{CDCl}_3$ ):  $\delta = 144.5$ , 132.7, 129.8, 127.9 (Ph-Ts), 97.3 (C-1), 71.5 (C-4), 68.5 (C-6), 69.4 (C-5), 68.5 (C-3), 67.3 (C-1'), 37.0 (C-2), 21.6 ( $\text{CH}_3$ -Ts), 31.9, 29.6, 29.6, 29.5, 29.4, 29.3, 26.1 (C-2' to C-11'), 14.1 (C-12') ppm.  $\text{C}_{25}\text{H}_{42}\text{O}_7\text{S}$  (486.27): calcd. C 61.70, H 8.70; found C 61.72, H 8.67.

**Dodecyl 2-Deoxy-6-O-tosyl- $\beta$ -D-arabino-hexopyranoside (13):** The above-mentioned procedure gave **13** as a syrup (0.66 g, 90.8%).  $\alpha_D^{20} = -5.1$  ( $c = 1$ ,  $\text{CH}_2\text{Cl}_2$ ).  $R_f = 0.50$  (1:1 EtOAc/cyclohexane).  $^1\text{H}$  NMR (400 MHz,  $\text{CDCl}_3$ ):  $\delta = 7.82$  (d, 2 H, Ph-Ts), 7.33 (d, 2 H, Ph-Ts), 4.49 (dd,  $^3J_{1,2a} = 9.6$ ,  $^3J_{1,2e} = 2.27$  Hz, 1 H, 1-H), 4.35–4.25 (m, 2 H, 6a-H, 6b-H), 3.69 (ddd,  $^3J_{1'a,2'a} = ^3J_{1'a,2'b} = 6.19$ ,  $^3J_{1'a,1'b} = 9.22$  Hz, 1 H, 1'a-H), 3.56 (m, 1 H, 3-H), 3.43–3.28 (m, 3 H, 4-H, 5-H, 1'b-H), 2.44 (s, 3 H,  $\text{CH}_3$ -Ts), 2.10 (dd,  $^2J_{2e,2a} = 12.88$ ,  $^3J_{2e,3} = 5.05$  Hz, 1 H, 2e-H), 1.57–1.48 (m, 3 H, 2a-H, 2'a-H, 2'b-H), 1.32–1.22 (m, 18 H, 3'a,b-H to 11'a,b-H), 0.88 (t,  $^3J_{11',12'} = 6.32$  Hz, 3 H, 12'-H) ppm.  $^{13}\text{C}$  NMR (100.62 MHz,  $\text{CDCl}_3$ ):  $\delta = 144.5$ , 132.7, 129.8, 127.9 (Ph-Ts), 99.3 (C-1), 69.8 (C-1'a), 69.0 (C-6), 71.1 (C-3), 71.3, 73.5 (C-4, C-5), 37.2 (C-2), 21.6 ( $\text{CH}_3$ -Ts), 31.9, 29.6, 29.5, 29.4, 29.3, 26.1 (C-2' to C-11'), 14.1 (C-12') ppm.  $\text{C}_{25}\text{H}_{42}\text{O}_7\text{S}$  (486.27): calcd. C 61.70, H 8.70; found C 61.72, H 8.67.

**General Procedure for the Deoxygenation Reaction:**  $\text{LiAlH}_4$  (10.2 mmol, 0.39 g) was added to a solution of the alkyl 2-deoxy-6-O-tosyl-D-arabino-hexopyranoside (2.9 mmol) in THF (44 mL) at 0 °C and the reaction mixture was stirred at room temp. for 72 h. Then EtOAc was added dropwise until no gas was formed, then ice flakes were added to dissolve the precipitate and finally  $\text{CH}_2\text{Cl}_2$  (50 mL) was added. The organic phase was washed with water, dried with sodium sulfate and evaporated in a rotavapor to give a residue that was purified by CC eluting with EtOAc/cyclohexane (5:1) to afford the final product.

**Octyl 2,6-Dideoxy- $\alpha$ -D-arabino-hexopyranoside (14):** The above-mentioned procedure gave **14** as a syrup (0.53 g, 70.0%).  $\alpha_D^{20} = +3.5$  ( $c = 1$ ,  $\text{CH}_2\text{Cl}_2$ ).  $R_f = 0.49$  (3:1 EtOAc/cyclohexane).  $^1\text{H}$  NMR (400 MHz,  $\text{CDCl}_3$ ):  $\delta = 4.81$  (d,  $^3J_{1,2a} = 3.03$  Hz, 1 H, 1-H), 3.87 (ddd,  $^3J_{3,4} = 9.35$ ,  $^3J_{3,2a} = 12.25$ ,  $^3J_{2e,3} = 5.30$  Hz, 1 H, 3-H), 3.64–3.57 (m, 2 H, 5-H, 1'a-H), 3.34 (dt,  $^3J_{1'b,2'b} = ^3J_{1'b,2'a} = 6.82$ ,  $^2J_{1'a,1'b} = 9.35$  Hz, 1 H, 1'b-H), 3.05 (t,  $^3J_{4,3} = ^3J_{4,5} = 9.35$  Hz, 1 H, 4-H), 2.10 (dd,  $^2J_{2e,2a} = 12.63$ ,  $^3J_{2e,3} = 5.30$  Hz, 1 H, 2e-H), 1.66 (td,  $^3J_{2a,3} = 12.25$ ,  $^2J_{2e,2a} = 12.63$ ,  $^3J_{1,2a} = 3.03$  Hz, 1 H, 2a-H), 1.60–1.53 (m, 2 H, 2'a-H, 2'b-H), 1.39–1.20 (m, 10 H, 3'a,b-H to 7'a,b-H, 6- $\text{CH}_3$ ), 0.88 (t,  $^3J_{7',8'} = 6.82$  Hz, 3 H, 8'-H) ppm.  $^{13}\text{C}$  NMR (100.62 MHz,  $\text{CDCl}_3$ ):  $\delta = 97.1$  (C-1), 77.7 (C-4), 68.9 (C-5), 67.5 (C-3), 67.4 (C-1'), 37.8 (C-2), 31.8, 29.4, 29.3, 29.2, 26.1, 22.6 (C-2' to C-7'), 17.7 (C-6), 14.0 (C-8') ppm.  $\text{C}_{14}\text{H}_{28}\text{O}_4$  (260.20): calcd. C 64.58, H 10.84; found C 64.56, H 10.85.

**Octyl 2,6-Dideoxy- $\beta$ -D-arabino-hexopyranoside (15):**<sup>[28]</sup> The above-mentioned procedure gave **15** as a white solid (0.54 g, 72.0%). M.p.

80 °C.  $\alpha_D^{20} = -4.4$  ( $c = 1$ ,  $\text{CH}_2\text{Cl}_2$ ).  $R_f = 0.45$  (3:1 EtOAc/cyclohexane).  $^1\text{H}$  NMR (400 MHz,  $\text{CDCl}_3$ ):  $\delta = 4.47$  (d,  $^3J_{1,2a} = 8.08$  Hz, 1 H, 1-H), 3.86 (ddd,  $^3J_{3,4} = 8.34$ ,  $^3J_{3,2e} = 2.53$ ,  $^3J_{3,2a} = 9.35$  Hz, 1 H, 3-H), 3.65–3.56 (m, 2 H, 5-H, 1'a-H), 3.43 (dt,  $^2J_{1'b,1'a} = 9.35$ ,  $^3J_{1'b,2'a} = ^3J_{1'b,2'b} = 7.07$  Hz, 1 H, 1'b-H), 3.10 (t,  $^3J_{4,3} = ^3J_{4,5} = 8.34$  Hz, 1 H, 4-H), 2.10 (dd,  $^3J_{3,2e} = 2.53$ ,  $^2J_{2e,2a} = 12.44$  Hz, 1 H, 1 H, 2e-H), 1.65–1.56 (m, 3 H, 2a-H, 2'a-H, 2'b-H), 1.35–1.23 (m, 13 H, 3'a,b-H to 7'a,b-H, 6- $\text{CH}_3$ ), 0.88 (t,  $^3J_{7',8'} = 5.81$  Hz, 3 H, 8'-H) ppm.  $^{13}\text{C}$  NMR (100.62 MHz,  $\text{CDCl}_3$ ):  $\delta = 99.5$  (C-1), 77.6 (C-5), 71.8 (C-4), 71.5 (C-3), 39.1 (C-1'), 31.8 (C-2), 29.7, 29.6, 29.4, 29.2, 26.0, 22.6 (C-2' to C-7'), 17.7 (C-6), 14.1 (C-8') ppm.  $\text{C}_{14}\text{H}_{28}\text{O}_4$  (260.20): calcd. C 64.58, H 10.84; found C 64.60, H 10.83.

**Dodecyl 2,6-Dideoxy- $\alpha$ -D-arabino-hexopyranoside (16):** The above-mentioned procedure gave **16** as a white solid (0.73 g, 79%). M.p. 36 °C.  $\alpha_D^{20} = +7.1$  ( $c = 1$ ,  $\text{CH}_2\text{Cl}_2$ ).  $R_f = 0.53$  (3:1 EtOAc/cyclohexane).  $^1\text{H}$  NMR (400 MHz,  $\text{CDCl}_3$ ):  $\delta = 4.81$  (d,  $^3J_{1,2a} = 2.78$  Hz, 1 H, 1-H), 3.88 (ddd,  $^3J_{3,2e} = 5.05$ ,  $^3J_{3,2a} = 11.87$ ,  $^3J_{3,4} = 10.36$  Hz, 1 H, 3-H), 3.65–3.59 (m, 2 H, 5-H, 1'a-H), 3.34 (dt,  $^3J_{1'b,2'b} = ^3J_{1'b,2'a} = 6.57$ ,  $^3J_{1'a,1'b} = 9.10$  Hz, 1 H, 1'b-H), 3.08–3.03 (m, 2 H, 4-H, 5-H), 2.10 (dd,  $^2J_{2e,2a} = 12.76$ ,  $^3J_{2e,3} = 5.05$  Hz, 1 H, 2e-H), 1.66 (td,  $^3J_{2a,3} = 11.87$  Hz, 1 H, 2a-H), 1.59–1.52 (m, 2 H, 2'a-H, 2'b-H), 1.39–1.20 (m, 21 H, 3'a,b-H to 11'a,b-H, 6- $\text{CH}_3$ ), 0.88 (t,  $^3J_{7',11'} = 7.33$  Hz, 3 H, 12'-H) ppm.  $^{13}\text{C}$  NMR (100.62 MHz,  $\text{CDCl}_3$ ):  $\delta = 97.1$  (C-1), 77.8 (C-4), 69.0 (C-5), 67.5 (C-3), 67.4 (C-1'), 37.8 (C-2), 31.8, 29.6, 29.6, 29.5, 29.4, 29.3, 26.1, 22.7 (C-2' to C-11'), 17.7 (C-6), 14.1 (C-12') ppm.  $\text{C}_{18}\text{H}_{36}\text{O}_4$  (316.26): calcd. C 68.31, H 11.47; found C 68.32, H 11.46.

**Dodecyl 2,6-Dideoxy- $\beta$ -D-arabino-hexopyranoside (17):** The above-mentioned procedure gave **17** as a white solid (0.69 g, 75.0%). M.p. 97 °C.  $\alpha_D^{20} = -4.5$  ( $c = 1$ ,  $\text{CH}_2\text{Cl}_2$ ).  $R_f = 0.50$  (3:1 EtOAc/cyclohexane).  $^1\text{H}$  NMR (400 MHz,  $\text{CDCl}_3$ ):  $\delta = 4.49$  (dd,  $^3J_{1,2a} = 9.6$ ,  $^3J_{1,2e} = 1.26$  Hz, 1 H, 1-H), 3.86 (dt,  $^3J_{1'a,1'b} = 9.22$ ,  $^3J_{1'a,2'a} = ^3J_{1'a,2'b} = 6.95$  Hz, 1 H, 1'a-H), 3.59 (ddd,  $^3J_{3,4} = 9.09$ ,  $^3J_{3,2e} = 2.02$ ,  $^3J_{3,2a} = 9.35$  Hz, 1 H, 3-H), 3.43 (dt,  $^3J_{1'b,1'a} = 9.22$ ,  $^3J_{1'b,2'a} = ^3J_{1'b,2'b} = 7.07$  Hz, 1 H, 1'b-H), 3.26 (dq,  $^3J_{5,6} = 6.44$ ,  $^3J_{5,4} = 9.09$  Hz, 1 H, 5-H), 3.09 (t,  $^3J_{5,4} = 9.09$  Hz, 1 H, 4-H), 2.21 (ddd,  $^3J_{1,2e} = 1.52$ ,  $^3J_{3,2e} = 2.02$ ,  $^2J_{2e,2a} = 12.88$  Hz, 1 H, 2e-H), 1.62–1.55 (m, 3 H, 2a-H, 2'a-H, 2'b-H), 1.35–1.24 (m, 21 H, 3'a,b-H to 11'a,b-H, 6- $\text{CH}_3$ ), 0.88 (t,  $^3J_{11',12'} = 6.82$  Hz, 3 H, 12'-H) ppm.  $^{13}\text{C}$  NMR (100.62 MHz,  $\text{CDCl}_3$ ):  $\delta = 99.5$  (C-1), 77.6 (C-5), 71.7 (C-4), 71.6 (C-3), 69.6 (C-1'), 39.1 (C-2), 31.9, 30.9, 29.6, 29.6, 29.5, 29.4, 29.3, 26.0 (C-2' to C-11'), 17.7 (C-6), 14.1 (C-12') ppm.  $\text{C}_{18}\text{H}_{36}\text{O}_4$  (316.26): calcd. C 68.31, H 11.47; found C 64.29, H 10.48.

**Surface Activity:** The surface tensions were determined with a Kruss K100MK2 automatic Interfacial Tensiometer using the du Noüy ring method at  $35.0 \pm 0.1$  °C. The du Noüy ring non-detachment technique was used and the surface tensions determined as a function of surfactant concentration following the experimental procedure described previously. The Harkins and Jordan correction was automatically introduced by the tensiometer.

Most aqueous solutions were prepared by weight in an A&D Instruments analytical balance to  $\pm 2 \times 10^{-5}$  g and the dissolution of the most concentrated solutions was accelerated by immersing the solutions in an ultrasound bath at 35 °C. The surface tensions were determined exclusively on clear isotropic solutions and the tensiometer calibration was checked with Milli-Q water before each run. The most dilute solutions exhibited a time-dependent surface tension that decreases on standing. Therefore all solutions were pre-equilibrated for at least 30 min prior to measurement. The surface tension values given in this work are the average of at least 10 independent evaluations and include an evaluation of solutions

prepared independently by weight and by successive dilution to cross-check the reliability of the experimental procedure.

**Antimicrobial Activity:** The antibacterial activities of the compounds were screened by using the paper disk diffusion method.<sup>[8]</sup> The tests were carried out with *Bacillus cereus* (ATCC 11778), *Bacillus subtilis* (ATCC 6633), *Enterococcus faecalis* (ATCC 29212), *Escherichia coli* (ATCC 8739), *Listeria monocytogenes* (ATCC 7644), *Pseudomonas aeruginosa* (ATCC 27853), *Salmonella enteritidis* (ATCC 13076) and *Staphylococcus aureus* (ATCC 25923). The culture medium and used for bacteria growth was Nutrient Agar incubated at 37 °C. Paper disks of 6.4 mm were placed on the agar and a solution of each substance (300 µg) in DMSO (15 µL) was applied to each disk. Chloramphenicol was used as a control. After incubation, the nearest diameter of the inhibition zone was measured and a compound was considered active at an inhibition diameter ≥11 mm. At least three replicates were made.

Subsequent tests to determine the minimal inhibition concentrations (MICs) were conducted on the compounds that exhibited considerable activity by the paper disk diffusion method. The broth dilution method<sup>[8]</sup> was used to test the susceptible microbes *B. subtilis*, *B. cereus*, *E. faecalis* and *L. monocytogenes*. Overnight cultures were also used. Serial dilutions starting at 500 µg/mL until 1.95 µg/mL were made for the compounds tested. Chloramphenicol dilutions ranged between 50 and 0.195 µg/mL. Bacteria were incubated at 35 °C for 16–20 h. At least three replicates were made.

The microbial susceptibility of *Bacillus anthracis* to the most active compounds was evaluated. Three strains from the collection of the Instituto Nacional de Saúde Doutor Ricardo Jorge, INSA, Portugal, were used in the tests: BA01, from sheep origin; BA02, human pathogen; BA03, vaccine strain. The assays were carried out in a biosafety level 3 laboratory by using the agar dilution method on the Müller–Hinton medium according to the Clinical and Laboratory Standards Institute (CLSI) guidelines.<sup>[29]</sup>

Serial dilutions from 256 to 1 µg/mL for each compound and the standard antibiotic chloramphenicol were prepared in DMSO. The plates were incubated overnight at 37 °C for 16 h. The MIC is defined as the lowest concentration of the tested compounds that inhibits bacterial growth.

**Anticholinesterase Activity:** The colorimetric Ellman's assay<sup>[30]</sup> was used to screen the in vitro anticholinesterase activities of compounds with a concentration of 100 µg/mL. The enzyme activity and enzyme inhibition were calculated from the change in the rate of absorbance with time ( $V = \Delta A/\Delta t$ ) data as follows:

$$\text{Enzyme inhibition [\%]} = 100 - \text{enzyme activity [\%]}$$

$$\text{Enzyme activity [\%]} = 100 \times V/V_{\max}$$

Maximum rates ( $V_{\max}$ ) were obtained when no inhibitor was used.  $V$  is the rate obtained in the presence of the inhibitor compound.

**Spectrophotometer and Chemicals:** A double-beam Shimadzu® spectrophotometer equipped with thermostatic cell holders was used in the visible range (425 nm) and operated in kinetic mode. The absorbance data were acquired with a personal computer using UV Probe software. Appropriate disposable plastic cuvettes were used in the kinetic experiments. For inhibition type assays, an automated 96-well microplate reader spectrophotometer (Perlong DNM-9602) with temperature control at 30 °C was used and measurements were made every minute for 4 minutes.

The reagents (p.a. quality) were purchased from Sigma–Aldrich: enzymes: AChE from bovine erythrocytes and BChE from human

serum; substrates: acetylthiocholine iodide (ATChI) and *S*-butyrylthiocholine iodide (BTChI) crystalline, and 5,5'-dithiobis(2-nitrobenzoic acid) (DTNB); reagents used for preparing buffers and solutions:  $\text{KH}_2\text{PO}_4$ , KOH,  $\text{NaHCO}_3$ . Deionized/sterilized water was used to prepare the pH 8.0 buffer, DTNB and test compound solutions.

**Solution Preparations:** Preparation of 0.1 M phosphate buffer (pH 8.0): Potassium dihydrogen phosphate (136.1 mg, 1 mmol) was dissolved in water (10 mL) and adjusted with potassium hydroxide to a pH of  $8.0 \pm 0.1$ . The buffer solution was freshly prepared and stored in the refrigerator.

AChE solution (1.32 U/mL): The enzyme (1.32 U) was diluted in freshly prepared pH 8.0 buffer until a final volume of 1 mL.

BChE solution (0.44 U/mL): The enzyme (0.44 U) was diluted in freshly prepared pH 8.0 buffer until a final volume of 1 mL.

DTNB solution (0.01 M): DTNB (3.96 mg, 0.01 mmol) was dissolved in water (1 mL) containing sodium hydrogen carbonate (1.5 mg).

ATChI and BTChI aqueous solutions (0.022 M) were prepared. All solutions were stored in Eppendorf caps (100 µL aliquots) in the refrigerator. Test compounds were prepared with a final concentration of 100 µg/mL in the reaction cuvette.

**AChE/BChE Activity Assay:** The buffer solution (200 µL) was added to the cuvette, followed by the enzyme solution (5 µL), DTNB (5 µL) and the test compound solution (5 µL). The reagents were carefully mixed and kept at 30 °C for 15 min in a heated water bath and then the substrate (5 µL) was added. The absorbance data was recorded during a reaction time of 4 min at 30 °C. At least four replicates were made. Blank assays without the enzyme or test compounds were performed to check for any non-enzymatic hydrolysis of the substrate.

The final concentrations of chemicals in the test were as follows: [AChE] = 0.03 U/mL, [BChE] = 0.01 U/mL, [Compound] = 100 µg/mL, [DTNB] = 0.0002273 M, [ATChI] = [BTChI] = 0.0005 M.

**Statistical Data Analysis:** The *t*-test (one sided) was carried out to evaluate whether the average inhibition of the enzymes by the new compounds (100 µg/mL) and the positive control donepezil (approved drug) are significantly higher than the average inhibition (0%) obtained in the assay without any inhibitor. The *t*-test gives a probability between 0.000 and 1.000. When the probability is ≤0.050 or 5% then the inhibition obtained with the extract at a certain concentration is significant.

**Determination of Inhibition Type and  $K_i$ :** To determine the inhibition type and inhibition constant ( $K_i$ ), the substrate concentration was varied between 0.03 and 0.13 mM for inhibitor concentrations between 0 and 1.65 mM.  $K_i$  was determined from the plot of  $K_m'/V'$  versus the inhibitor concentration, for which  $K_m'$  is the apparent  $K_m$  and  $V'$  is the apparent  $V$ . The intercept of the resulting straight line with the inhibitor axis is  $-K_i$ .

**Computational Methods:** Coordinates for the proteins were retrieved from the Protein Data Bank (butyrylcholinesterase, BChE: 1P0I;<sup>[26]</sup> acetylcholinesterase, AChE: 1B41<sup>[27]</sup>). The files were clean from everything except the protein (water, ligands and other small molecules were all removed). There were some missing residues, but these were located far away from the active site pocket and were not corrected. The artificial terminals hence generated in the polypeptide chain were, for simplicity, treated as neutral terminals. The modelled deoxy glycoside ligands were built by using PyMOL.<sup>[31]</sup> Each molecule was geometrically optimized with Gaussian 03<sup>[32]</sup> by using the B3LYP functional and 6-31G(d,p) basis sets.<sup>[33,34]</sup> The

optimized conformations were used in the docking calculations with AutoDockVina.<sup>[35]</sup>

All possible bonds were allowed to rotate freely by including the respective ligand torsions in the calculation using AutoDock Tools.<sup>[36]</sup> This results in 10 rotatable bonds for ligands **6** and **7**, and 12 for ligands **14** and **15** (see Scheme 1 for structures). The AutoDockVina search space was defined as a cubic box centred at the active site with a size large enough to include one shell of residues around the cavity. The “exhaustiveness” parameter was set to 16 and 500 AutoDockVina runs were performed to obtain finally around 10000 solutions. The AutoDockVina search method was the “iterative local search global optimizer”. Both proteins were considered as rigid receptors without any kind of flexibility. The non-polar hydrogen atoms from the protein and ligands were merged. The cluster analysis was performed by using the *g\_cluster* tool from GROMACS<sup>[37,38]</sup> with the Jarvis–Patrick method and an RMSD cutoff of 0.8 Å.

**Supporting Information** (see footnote on the first page of this article): Copies of NMR spectra for new compounds.

## Acknowledgments

The authors thank the Management Authorities of the European Regional Development Fund and the National Strategic Reference Framework for the support of the Incentive System – Research & Technological Development Co-Promotion Project nr. 21457. The Fundação para a Ciência e a Tecnologia (FCT) is gratefully acknowledged for a post-doctoral research grant (grant number BPD/42567/2007) and for the financial support of the CQB Strategic Project PEst-OE/QUI/UI0612/2011.

- [1] I. Rico-Lattes, *Actual. Chim.* **2007**, *305*, 3–11.
- [2] V. Neto, R. Granet, P. Krausz, *Tetrahedron* **2010**, *66*, 4633–4646.
- [3] S. Schreier, S. V. P. Malheiros, E. de Paula, *Biochim. Biophys. Acta – Biomembranes* **2000**, *1508*, 210–234.
- [4] I. M. Banat, A. Franzetti, I. Gandolfi, G. Bestetti, M. G. Martinotti, L. Fracchia, T. J. Smyth, R. Marchant, *Appl. Microbiol. Biotechnol.* **2010**, *87*, 427–444.
- [5] J. G. Eley, P. Triumalashetty, *AAPS PharmSciTech* **2001**, *2*, E19.
- [6] M. A. Rosenow, C. L. Magee, J. C. Williams, J. P. Allen, *Acta Crystallogr., Sect. D: Biol. Crystallogr.* **2002**, *58*, 2076–2081.
- [7] K. Holmberg (Ed.), *Novel Surfactants. Preparation, Applications and Biodegradability*, 2nd ed., Surfactant Science Series, Marcel Dekker, New York, **2003**, vol. 114, pp. 1–192.
- [8] F. V. M. Silva, M. Goulart, J. Justino, A. Neves, F. Santos, J. Caio, S. Lucas, A. Newton, D. Sacoto, E. Barbosa, M. S. Santos, A. P. Rauter, *Bioorg. Med. Chem.* **2008**, *16*, 4083–4092.
- [9] A. P. Rauter, S. Lucas, T. Almeida, D. Sacoto, V. Ribeiro, J. Justino, A. Neves, F. V. M. Silva, M. C. Oliveira, M. J. Ferreira, M. S. Santos, E. Barbosa, *Carbohydr. Res.* **2005**, *340*, 191–201.
- [10] E. Helgason, O. A. Okstad, D. A. Caugant, H. A. Johansen, A. Fouet, M. Mock, I. Hegna, A. B. Kolsto, *Appl. Environ. Microbiol.* **2000**, *66*, 2627–2630.
- [11] B. Nammalwar, R. A. Bunce, K. D. Berlin, C. R. Bourne, P. C. Bourne, E. Barrow, W. W. Barrow, *Eur. J. Med. Chem.* **2012**, *54*, 387–396.
- [12] A. Louie, B. D. VanScoy, D. L. Brown, R. W. Kulawy, H. S. Henry, G. L. Drusano, *Antimicrob. Agents Chemother.* **2012**, *56*, 1229–1239.
- [13] A. P. Rauter, A. Martins, J. Caio, J. P. Pais, P. Serra, M. S. Santos, A. Pelerito, J. P. Gomes, J. Justino, R. Dias, R. Tenreiro, PCT/IB2012/050123, **2012**, patent submitted.
- [14] P. D. Sloane, S. Zimmerman, C. Suchindran, P. Reed, L. Wang, M. Boustani, S. Sudha, *Annu. Rev. Public Health* **2002**, *23*, 213–231.
- [15] Y. J. Woo, B. H. Lee, G. H. Yeun, H. J. Kim, J. M. Ko, M.-H. Won, B. H. Lee, J. H. Park, *Bull. Korean Chem. Soc.* **2011**, *32*, 2997–3002.
- [16] N. H. Greig, T. Utsuki, D. K. Ingram, Y. Wang, G. Pepeu, C. Scali, Q.-S. Yu, J. Mamczarz, H. W. Holloway, T. Giordano, D. Chen, K. Furukawa, K. Sambamurti, A. Brossi, D. Lahiri, *Proc. Natl. Acad. Sci. USA* **2005**, *102*, 17213–17218.
- [17] Y. Furukawa-Hibi, T. Alkam, A. Nitta, A. Matsuyama, H. Mizoguchi, K. Suzuki, S. Moussaoui, Q. S. Yu, N. H. Greig, T. Nagai, K. Yamada, *Behav. Brain Res.* **2011**, *225*, 222–229.
- [18] A. P. Rauter, T. Almeida, A. I. Vicente, V. Ribeiro, J. C. Bordado, J. P. Marques, F. Ramôa-Ribeiro, M. J. Ferreira, C. Oliveira, M. Guisnet, *Eur. J. Org. Chem.* **2006**, *10*, 2429–2439.
- [19] K. Shinoda, T. Yamaguchi, R. Hori, *Bull. Chem. Soc. Jpn.* **1961**, *34*, 237–241.
- [20] I. Soderberg, C. J. Drummond, D. N. Furlong, S. Godkin, B. Matthews, *Colloids Surf., A: Physicochem. Eng. Asp.* **1995**, *102*, 91–97.
- [21] S. Matsumura, K. Imai, S. Yoshikawa, K. Kawada, T. Uchibori, *J. Am. Oil Chem. Soc.* **1990**, *67*, 996–1001.
- [22] B. J. Boyd, C. J. Drummond, I. Krodkiewska, F. Grieser, *Langmuir* **2000**, *16*, 7359–7367.
- [23] M. G. Bonicelli, G. F. Ceccaroni, C. La Mesa, *Colloid Polym. Sci.* **1998**, *276*, 109–116.
- [24] J. Israelachvili, *Intermolecular and Surface Forces*, 2nd ed. Academic Press, Suffolk, **1998**, p. 450.
- [25] J. Bernstein, R. J. Davey, J. Henck, *Angew. Chem.* **1999**, *111*, 3646; *Angew. Chem. Int. Ed.* **1999**, *38*, 3440–3461.
- [26] Y. Nicolet, O. Lockridge, P. Masson, J. C. Fontecilla-Camps, F. Nachon, *J. Biol. Chem.* **2003**, *278*, 41141–41147.
- [27] G. Kryger, M. Harel, K. Giles, L. Toker, B. Velan, A. Lazar, C. Kronman, D. Barak, N. Ariel, A. Shafferman, I. Silman, J. L. Sussman, *Acta Crystallogr., Sect. D: Biol. Crystallogr.* **2000**, *56*, 1385–1394.
- [28] K. Toshima, K. Inagaki, M. Nakata, S. Matsumura, *Synlett* **1997**, *6*, 695–696.
- [29] *CLSI, Methods for Dilution Antimicrobial Susceptibility Tests for Bacteria that Grow Aerobically: Approved Standard*, 4th ed., NCCLS Document M7-A4, **1997**.
- [30] G. L. Ellman, D. K. Courtney, V. Andres, R. M. Featherstone, *Biochem. Pharmacol.* **1961**, *7*, 88–95.
- [31] *The PyMOL Molecular Graphics System*, v. 1.4r1, Schrodinger, LLC, **2010**.
- [32] M. J. Frisch, G. W. Trucks, H. B. Schlegel, G. E. Scuseria, M. A. Robb, J. R. Cheeseman, J. A. Montgomery, Jr., T. Vreven, K. N. Kudin, J. C. Burant, J. M. Millam, S. S. Iyengar, J. Tomasi, V. Barone, B. Mennucci, M. Cossi, G. Scalmani, N. Rega, G. A. Petersson, H. Nakatsuji, M. Hada, M. Ehara, K. Toyota, R. Fukuda, J. Hasegawa, M. Ishida, T. Nakajima, Y. Honda, O. Kitao, H. Nakai, M. Klene, X. Li, J. E. Knox, H. P. Hratchian, J. B. Cross, V. Bakken, C. Adamo, J. Jaramillo, R. Gomperts, R. E. Stratmann, O. Yazyev, A. J. Austin, R. Cammi, C. Pomelli, J. W. Ochterski, P. Y. Ayala, K. Morokuma, G. A. Voth, P. Salvador, J. J. Dannenberg, V. G. Zakrzewski, S. Dapprich, A. D. Daniels, M. C. Strain, O. Farkas, D. K. Malick, A. D. Rabuck, K. Raghavachari, J. B. Foresman, J. V. Ortiz, Q. Cui, A. G. Baboul, S. Clifford, J. Cioslowski, B. B. Stefanov, G. Liu, A. Liashenko, P. Piskorz, I. Komaromi, R. L. Martin, D. J. Fox, T. Keith, M. A. Al-Laham, C. Y. Peng, A. Nanayakkara, M. Challacombe, P. M. W. Gill, B. Johnson, W. Chen, M. W. Wong, C. Gonzalez, J. A. Pople, *Gaussian 03*, Revision C.02, Gaussian, Inc., Wallingford, CT, **2004**.
- [33] A. Becke, *Phys. Rev. A* **1988**, *38*, 3098–3100.
- [34] C. Lee, W. Yang, R. Parr, *Phys. Rev. B* **1988**, *37*, 785–789.

- [35] O. Trott, A. J. Olson, *J. Comput. Chem.* **2010**, *31*, 455–461.
- [36] G. M. Morris, R. Huey, W. Lindstrom, M. F. Sanner, R. K. Belew, D. S. Goodsell, A. J. Olson, *J. Comput. Chem.* **2009**, *30*, 2785–2791.
- [37] D. van Der Spöel, E. Lindahl, B. Hess, G. Groenhof, A. E. Mark, H. J. C. Berendsen, *J. Comput. Chem.* **2005**, *26*, 1701–1718.
- [38] B. Hess, C. Kutzner, D. van Der Spöel, E. Lindahl, *J. Chem. Theory Comput.* **2008**, *4*, 435–447.

Received: November 13, 2012

Published Online: February 18, 2013